Measurement of dielectric properties (mHz - MHz) of sedimentary rocks

Qifei Niu and Manika Prasad, Department of Petroleum Engineering, Colorado School of Mines*

Summary

The dielectric property is a useful parameter that can be used to infer other properties of porous media such as water saturation, permeability, etc. The dielectric properties (mHz to MHz) of isotropic porous media have been extensively studied. However, related studies are very rare for anisotropic porous media. In this study, we have measured the directional dielectric spectra of two sedimentary rocks (one Bakken shale sample and one Lyons sandstone sample) using the combination of 2- and 4- electrode methods in the frequency range between 10^{-3} and 10^{7} Hz. It is shown that the dielectric constant of these two samples generally increases as the frequency decreases. This is because, as the frequency decreases, more polarization mechanisms start to contribute to the measured dielectric constant. It is also shown that the dielectric anisotropy in these samples decreases as the frequency increases, indicating that different polarization mechanisms induce different degrees of dielectric anisotropy.

Introduction

The permittivity (or dielectric constant) is an important property for porous media, which quantifies the energy storage in the material when an electric field is applied. The dielectric constant of a porous media is strongly related to the frequency (time scale) because the polarization at different frequencies is controlled by different length scales (see a review in Chelidze & Gueguen, 1999; Chelidze *et al.*, 1999). The dielectric constant of porous media is also related to the relative fractions of the solid, liquid, and gaseous phases, as well as the spatial distribution of each phase (e.g., see Friedman, 1998). Compared to other parameters, the chemical composition of the solid phase has less influence on the dielectric constant because most minerals have a low dielectric constant (Telford *et al.*, 1990).

For geological sediments such as rocks and soils, the high-frequency (>MHz) dielectric measurement has been used frequently to infer the water content/saturation information in both laboratory, borehole and field conditions (Robinson *et al.*, 2003). The underlying physics is that water and minerals have a distinct dielectric contrast at high frequency, ~80 for water and ~5 for minerals. Moreover, the salinity influence on the dielectric constant of water is insignificant, making the dielectric measurement superior to the electrical conductivity measurement for water content determination.

The low-frequency (<10 kHz) dielectric measurement is usually known as spectral induced polarization (SIP) method in geophysical community. In the past few decades, induced polarization has been shown to be a very promising geophysical tool in environmental geosciences and in hydrogeophysics for a broad number of applications including permeability estimation (e.g., Binley *et al.*, 2005), the characterization of the near-surface lithology (Gazoty et al., 2012b), the detection of microbial growth in porous media (Davis *et al.*, 2006), landfill characterization (Gazoty *et al.*, 2012a) and the delineation of contaminant plumes (Deceuster & Kaufmann, 2012).

In this paper, the dielectric property (mHz to MHz) of anisotropic sedimentary rocks is experimentally studied. We first briefly introduce the polarization mechanisms and related theoretical models. Two samples, one Bakken shale sample and one Lyons sandstone sample, are measured using two- and four-electrode methods with an impedance analyzer and a SIP system. The measured results are presented, and related discussions are also included.

Polarization mechanisms

In the frequency range between mHz and MHz, there are mainly three polarization mechanisms related to the dielectric properties of porous media saturated with electrolyte: interfacial polarization, membrane polarization, and electrical double layer polarization. In this section, we briefly introduce these mechanisms and associated theoretical models.

Maxwell-Wagner Polarization (MWP)

The Maxwell-Wagner polarization or interfacial polarization is caused by the formation of field-induced free charge distributions near the interface between different phases of porous materials or colloidal suspensions (Maxwell, 1892; Wagner, 1914). Models based on the effective medium approximation (e.g., Hanai, 1960; Sen *et al.*, 1981) are efficient in modeling this contribution. For anisotropic materials, the following differential effective medium (DEM) theory based model is used to describe the dielectric constant of anisotropic sedimentary rocks. The model reads as follows,

$$\frac{\varepsilon-\varepsilon_s}{\varepsilon_w-\varepsilon_s}\left(\frac{\varepsilon_w}{\varepsilon}\right)^{L_i}=\phi \quad (1)$$

where ε, ε_w, and ε_s are the dielectric constants of the material, water, and solid particle, respectively. The

parameter L_i is the depolarization factor in the direction i, and ϕ is the porosity of the material.

MWP can be regarded as a scaling law, which calculates the effective dielectric constant of a composite based on the relative fraction and dielectric constant of each phase. In equation (1), the dielectric constant of the solid particle is not only from the intrinsic permittivity (i.e., from electronic/atomic polarization) of the particle but also from the contribution of membrane polarization/electrical double layer polarization. Note that the membrane/electrical double layer polarization results from the interface between the solid and liquid phases. Compared with pore/solid phase, the volume of the interface is insignificant. In practice, the permittivity contribution from the interface is usually averaged over the solid phase so that the solid phase has an increase in the dielectric constant in addition to its intrinsic dielectric property.

Membrane Polarization (MP)

In the intermediate frequency range, the membrane polarization (MP) can contribute to the dielectric properties of a porous medium (Marshall & Madden, 1959). In MP, the material is modelled by wide pores and narrow pore throats as shown in Figure 1. The surface of both pores and pore throats is negatively charged. In the pores, the electrical double layer (EDL) is formed and it only occupies a small portion of the pore space. The dielectric properties induced by the EDL polarization will be discussed in the next subsection.

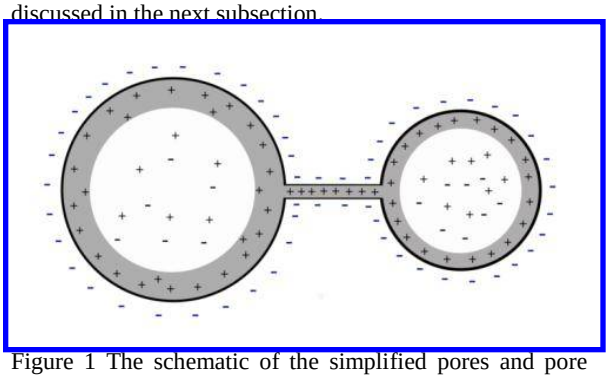

Figure 1 The schematic of the simplified pores and pore throats in a porous media.

For the narrow pore throat as shown in Figure 1, the EDL also forms at the interface between liquid and solid phases, but it occupies a noticeable portion in the pore throat space. For example, Figure 1 shows an extreme case, in which the EDL occupies the entire space of the pore throat. In the pore throat, only cations can pass through but anions cannot. Therefore, the pore throat behaves an ion-selective or membrane-like property.

When subjected to an external electric field, an ion concentration gradient builds up, resulting in a frequency-dependent dielectric property. According to recent work (Bücker & Hördt, 2013b), the frequency-dependent dielectric can be modelled by a Cole-Cole model with frequency exponent c = 0.5 if the length of the pore throat is relative short. It should be noted that the current model for MP is still not mature enough to quantitatively describe the permittivity of porous media, and the related model parameters cannot be related to some petrophsyical properties of the material. In this study, we do not include the details of the theoretical model that is used to calculate the membrane polarization. One can refer to Bücker & Hördt (2013a) and Bücker & Hördt (2013b) for more information.

Electrical double layer polarization (EDLP)

We first review the basic concepts of the electrical double layer in porous media. Here we consider a rock saturated with electrolyte (Figure 2). As discussed in Figure 1, the pore is connected to the other pore spaces by pore throat(s). The radius of a pore is assumed to be larger than the radii of the pore throats. The surface of the solid (mineral) phase is considered to be negatively charged. The negative charges are counterbalanced by positive charges in the Stern and diffuse layers.

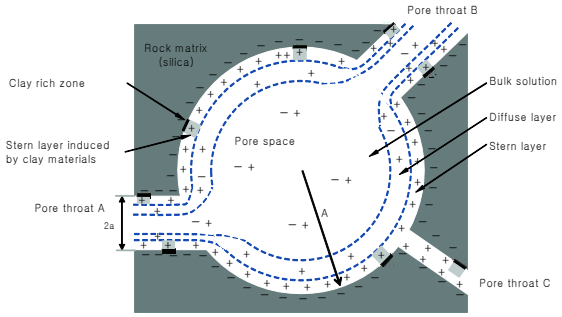

Figure 2 The schematic of the electrical double layer in the interface between the pore fluid and mineral (modified from Niu and Revil, 2016).

At low frequencies (usually <kHz), the governing polarization mechanism is the electrical double layer polarization (EDLP), which occurs at the liquid-solid interface in large pores (>1 μm) in the material (Revil, 2012). The dielectric response of a single spherical pore/particle induced by EDLP can be modelled by a Debye model. The characteristic relaxation time τ_{EDLP} for EDLP is related to the pore/particle radius r by the following equation (Niu & Revil, 2016),

$$\tau_{EDLP} = \frac{r^2}{2D_{(+)}^S} \quad (2)$$

where $D_{(+)}^S$ is the diffusion coefficient of the cations in the electrical double layer.

The maximum change in the dielectric constant ε_{EDLP} induced by EDLP is controlled by the specific surface conductance of the material by

$$\varepsilon_{EDLP} = \frac{2}{\Pi} \cdot \frac{\Sigma_S''}{\omega \varepsilon_0} \quad (3)$$

where Π is a characteristic particle size (Niu *et al.*, 2015), ω is the angular frequency, ε_0 is the permittivity of the free space, and Σ_S'' is the imaginary part of the specific surface conductance. For spherical particles, Π is the radius of the particle; for ellipsoid, Π is related to the aspect ratio, semi-major and minor axis lengths of the particle (Dukhin & Shilov, 1980).

Influence of pore/pore throat size

For porous medium with a pore size distribution $f(r)$, the dielectric constant of the material induced by EDLP can be obtained by the convolution of the pore size distribution with the dielectric response obtained for a delta distribution of pore size according to superposition principle (e.g., see Lesmes & Morgan, 2001; Leroy *et al.*, 2008; Niu & Revil, 2016). The dielectric constant induced by MP can also be obtained by considering the pore throat size distribution $g(r)$, which is similar to the convolution of pore size distribution in modelling EDLP (Bairlein *et al.*, 2016). However, this idea has never been explored partly because the theory of MP is still not mature enough for quantitative analysis.

Experiments

The dielectric constant of two samples, one Bakken shale and one Lyons sandstone, was measured in the frequency range between 10^{-3} Hz and 10^{-7} Hz. In order to measure the anisotropic dielectric properties, the samples were cut along directions parallel (||) and perpendicular ($\perp$) to the bedding plane. For frequencies ranging between 10^{-3} Hz to 10^{2} Hz, the four-electrode method (see Figure 3) and a SIP system were employed to conduct the measurement. Silver paste was used to inject the current into the sample. The non-polarized Ag-AgCl electrodes were used to measure the potential on the sample surface for the purpose to eliminate the electrode polarization. The measured impedance and phase shift were used to calculate the dielectric constant of the sample by considering the geometry of the sample and positions of the potential electrodes.

For frequency ranging between 10^{2} Hz to 10^{7} Hz, the two-electrode method (see Figure 3) and an impedance analyzer were used to conduct the measurement. We used silver paste as the electrodes, and the measured impedance and the phase shift were used to calculate the dielectric constant according to the geometry of the sample. The combination of two- and four-electrode methods has been used frequently to determine the broadband dielectric constant of sediments (Klein & Santamarina; Lesmes & Morgan, 2001). However, the broadband dielectric properties of anisotropic sedimentary rocks are rarely measured using this technique.

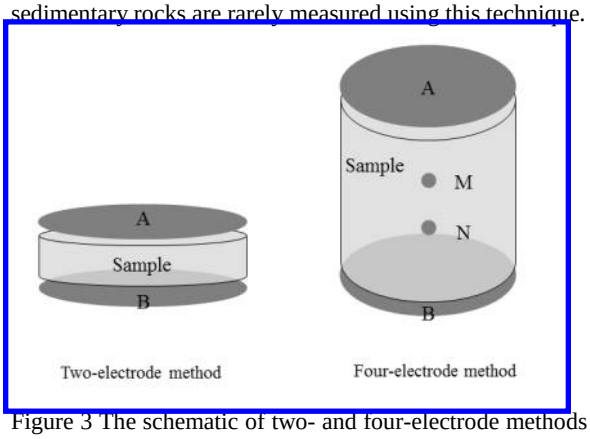

Figure 3 The schematic of two- and four-electrode methods used in the experiment in determining the dielectric properties of anisotropic sedimentary rocks.

Results

The measured directional dielectric constant of the two samples is shown in Figures 4 and 5. In general, the dielectric constant measured using 2- and 4-electrode methods agrees with each other very well, indicating that the influence of electrode polarization is not significant. It is noticed that the dielectric measured using 4-electrode method is not reliable at frequencies higher than kHz (e.g., see the data in the box in Figures 4 and 5). The error is known from the electromagnetic coupling between cables.

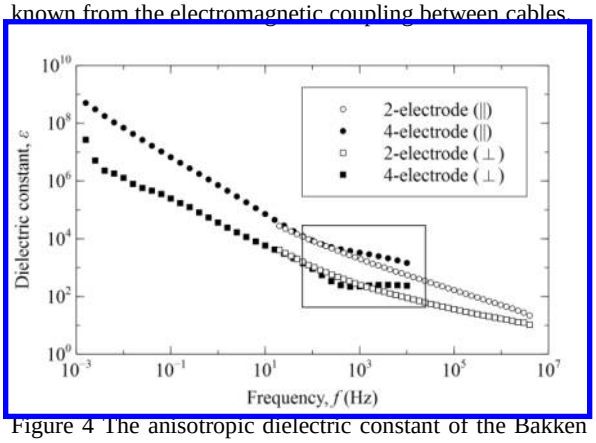

Figure 4 The anisotropic dielectric constant of the Bakken shale sample. The data from 4-electrode method in the box are not reliable because of the electromagnetic coupling between cables.

It is shown in Figures 4 and 5 that the dielectric constant increases when the frequency decreases for both directions (|| and $\perp$). This is because at high frequencies (>10^{6} Hz), which corresponds to a small length scale, only dipole/atomic/electronic polarizations contribute to the

measurement. While the frequency decreases (length scale increases), other polarization mechanisms, such as MP and EDLP, start to contribute to measured dielectric constant. At mHz range, the dielectric constant of the samples increase to ~ 10^8, indicting a strong influence of the EDLP and MP if we consider the fact that the dielectric constant at MHz is only ~10. It is also shown in Figures 4 and 5 that the dielectric constant measured at the direction parallel to the bedding plane is always larger than that from the direction perpendicular to bedding for the entire frequency range, indicating a significant anisotropy. In the next section, we discuss how the anisotropy varies with the frequency.

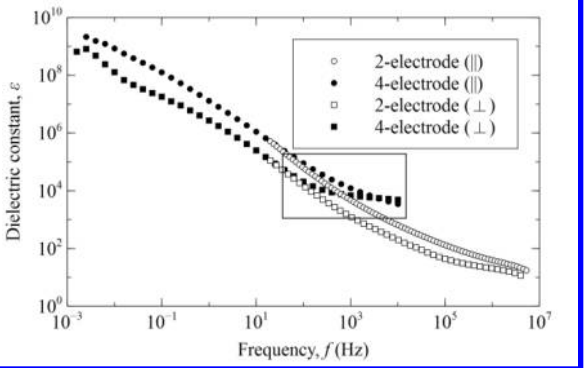

Figure 5 The anisotropic dielectric constant of the Lyons sandstone sample. The data from 4-electrode method in the box are not reliable because of the electromagnetic coupling between cables.

Anisotropy

As shown in Figures 4 and 5, the anisotropy in the dielectric constant is very clear for both samples in the frequency range between mHz and MHz. To clearly show the anisotropy, the anisotropic ratio of the two samples is plotted in Figure 6. At very low frequencies (on the left side of the solid lines in Figure 6), there is a decrease in the anisotropy ratio as the frequency decreases. This decrease might be due to the low-frequency experimental error because at low frequencies, the dielectric measurement usually takes hours, during which the sample may loss some pore water.

In general, the anisotropy of the two samples increases as the frequency decreases, indicating that different polarization mechanisms induce different degree of anisotropy in the dielectric properties. At low frequencies, the anisotropy is quite large (~50 for Bakken shale and ~ 7 for Lyons sandstone). Since at this frequency range, the EDLP dominates, the results mean that EDLP is strongly influenced by the spatial arrangement of the particles/pores. This is understandable because EDLP occurs in the interface between pores and solid particles, and the spatial distribution of the interface is governed by the spatial arrangement of particles/pores.

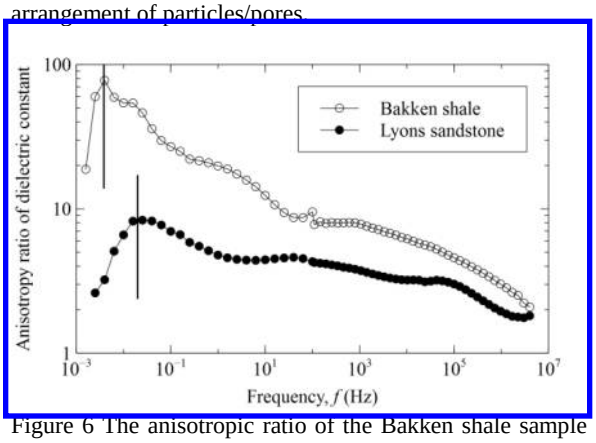

Figure 6 The anisotropic ratio of the Bakken shale sample and the Lyons sandstone sample in the frequency range between mHz to MHz.

The anisotropy ratio at intermediate frequency (10^2-10^5 Hz) is relative low (~10 for Bakken shale sample and ~5 for the Lyons sandstone sample). In this frequency range, the MP, which is governed by the narrow pore throat, dominates the dielectric measurement. The relative low anisotropy means the difference in the pore throat distribution in directions parallel and perpendicular to the bedding is not as significant as that for pore space, which governs the EDLP.

When the frequency reaches ~ 10^7 Hz, the anisotropy ratio for both samples decreases to ~2. At this frequency, the anisotropy is mainly from the interfacial layer polarization as described by Equation 1. For different directions, the depolarization factor L is different. Different L values are responsible for the dielectric anisotropy in high frequencies (> 10^6 Hz).

Conclusion

The study shows that the dielectric constant of sedimentary rocks generally increase as the frequency decreases due to more polarization mechanisms contributing to dielectric measurements. The anisotropy in the dielectric properties decreases as the frequency increases, indicating that different polarization mechanisms induce different degree of anisotropy. Among all the polarization mechanisms, electrical double layer polarization induces the most significant dielectric anisotropy.

Acknowledgements

The author is grateful to the OCLASSH consortium in Colorado School of Mines for the financial support.

EDITED REFERENCES

Note: This reference list is a copyedited version of the reference list submitted by the author. Reference lists for the 2016 SEG Technical Program Expanded Abstracts have been copyedited so that references provided with the online metadata for each paper will achieve a high degree of linking to cited sources that appear on the Web.

REFERENCES

Bairlein, K., M. Bücker, A. Hördt, and B. Hinze, 2016, Temperature dependence of spectral induced polarization data: Experimental results and membrane polarization theory: Geophysical Journal International, **205**, 440–453, http://dx.doi.org/10.1093/gji/ggw027.

Binley, A., L. D. Slater, M. Fukes, and G. Cassiani, 2005, Relationship between spectral induced polarization and hydraulic properties of saturated and unsaturated sandstone: Water Resources Research, **41**, W12417, http://dx.doi.org/10.1029/2005WR004202.

Bücker, M., and A. Hördt, 2013a, Analytical modelling of membrane polarization with explicit parametrization of pore radii and the electrical double layer: Geophysical Journal International, **194**, 804–813, http://dx.doi.org/10.1093/gji/ggt136.

Bücker, M., and A. Hördt, 2013b, Long and short narrow pore models for membrane polarization: Geophysics, **78**, no. 6, E299–E314, http://dx.doi.org/10.1190/geo2012-0548.1.

Chelidze, T. L., and Y. Gueguen, 1999, Electrical spectroscopy of porous rocks: A review — I. Theoretical models: Geophysical Journal International, **137**, 1–15, http://dx.doi.org/10.1046/j.1365-246x.1999.00799.x.

Chelidze, T. L., Y. Gueguen, and C. Ruffet, 1999, Electrical spectroscopy of porous rocks: a review — II. Experimental results and interpretation: Geophysical Journal International, **137**, 16–34, http://dx.doi.org/10.1046/j.1365-246x.1999.00800.x.

Davis, C. A., E. Atekwana, E. Atekwana, L. D. Slater, S. Rossbach, and M. R. Mormile, 2006, Microbial growth and biofilm formation in geologic media is detected with complex conductivity measurements: Geophysical Research Letters, **33**, L18403, http://dx.doi.org/10.1029/2006GL027312.

Deceuster, J., and O. Kaufmann, 2012, Improving the delineation of hydrocarbon-impacted soils and water through induced polarization (IP) tomographies: A field study at an industrial waste land: Journal of Contaminant Hydrology, **136**–**137**, 25–42, http://dx.doi.org/10.1016/j.jconhyd.2012.05.003.

Dukhin, S. S., and V. N. Shilov, 1980, Kinetic aspects of electrochemistry of disperse systems. Part II. Induced dipole moment and the non-equilibrium double layer of a colloid particle: Advances in Colloid and Interface Science, **13**, 153–195, http://dx.doi.org/10.1016/0001-8686(80)87005-9.

Friedman, S. P., 1998, A saturation degree-dependent composite spheres model for describing the effective dielectric constant of unsaturated porous media: Water Resources Research, **34**, 2949–2961, http://dx.doi.org/10.1029/98WR01923.

Gazoty, A., G. Fiandaca, J. Pedersen, E. Auken, and A. V. Christiansen, 2012a, Mapping of landfills using time-domain spectral induced polarization data: the Eskelund case study: Near Surface Geophysics, **10**, 575–586.

Gazoty, A., G. Fiandaca, J. Pedersen, E. Auken, A. V. Christiansen, and J. K. Pedersen, 2012b, Application of time domain induced polarization to the mapping of lithotypes in a landfill site: Hydrology and Earth System Sciences, **16**, 1793–1804, http://dx.doi.org/10.5194/hess-16-1793-2012.

Hanai, T., 1960, Theory of the dielectric dispersion due to the interfacial polarization and its application to emulsions: Kolloid-Zeitschrift, **171**, 23–31, http://dx.doi.org/10.1007/BF01520320.

Klein, K., and J. Santamarina, 1997, Methods for broad-band dielectric permittivity measurements (soil-water mixtures, 5 Hz to 1.3 GHz): Geotechnical Testing Journal, **20**, 168–178, http://dx.doi.org/10.1520/GTJ10736J.
Leroy, P., A. Revil, A. Kemna, P. Cosenza, and A. Ghorbani, 2008, Complex conductivity of water-saturated packs of glass beads: Journal of Colloid and Interface Science, **321**, 103–117, http://dx.doi.org/10.1016/j.jcis.2007.12.031.
Lesmes, D. P., and F. D. Morgan, 2001, Dielectric spectroscopy of sedimentary rocks: Journal of Geophysical Research. Solid Earth, **106**, 13329–13346, http://dx.doi.org/10.1029/2000JB900402.
Marshall, D. J., and T. R. Madden, 1959, Induced polarization, a study of its causes: Geophysics, **24**, 790–816, http://dx.doi.org/10.1190/1.1438659.
Maxwell, J. C., 1892, A treatise on electricity and magnetism, 3rd ed.: Clarendon press.
Niu, Q., M. Prasad, A. Revil, and M. Saidian, 2015, Textural control on the quadrature conductivity of porous media: Geophysics, **75**, no. 4, http://dx.doi.org/10.1190/1.3479835.
Niu, Q., and A. Revil, 2016, Connecting complex conductivity spectra to mercury porosimetry of sedimentary rocks: Geophysics, **81**, no. 1, E17–E32, http://dx.doi.org/10.1190/geo2015-0072.1.
Revil, A., 2012, Spectral induced polarization of shaly sands: Influence of the electrical double layer: Water Resources Research, **48**, W02517, http://dx.doi.org/10.1029/2011WR011260.
Robinson, D. A., S. B. Jones, J. M. Wraith, D. Or, and S. P. Friedman, 2003, A review of advances in dielectric and electrical conductivity measurement in soils using time domain reflectometry: Vadose Zone Journal, **2**, 444, http://dx.doi.org/10.2136/vzj2003.4440.
Sen, P. N., C. Scala, and M. H. Cohen, 1981, A self-similar model for sedimentary rocks with application to the dielectric constant of fused glass beads: Geophysics, **46**, 781–795, http://dx.doi.org/10.1190/1.1441215.
Telford, W. M., L. P. Geldart, and R. E. Sheriff, 1990, Applied geophysics, 2nd ed.: Cambridge University Press, http://dx.doi.org/10.1017/CBO9781139167932.
Wagner, K. W., 1914, Erklärung der dielektrischen Nachwirkungsvorgänge auf Grund Maxwellscher Vorstellungen: Archiwum Elektrotechniki, **2**, 371–387, http://dx.doi.org/10.1007/BF01657322.